Electronic Supplementary Material (ESI) for Chemical Communications.

Supporting Information

G-quadruplex ligands exhibit differential G-tetrad selectivity

Daniel D. Le, Marco Di Antonio, Louis K. M. Chan, and Shankar Balasubramanian

Table of contents

Table S1:

Oligo name	Oligo origin	Nucleic acid	Sequence (modification in bold)	Supplier
5'Cy5_hTelo	Human telomer	DNA	**Cy5**-AGG GTT AGG GTT AGG GTT AGG GT	Biomers
3'Cy5_hTelo	Human telomer	DNA	AGG GTT AGG GTT AGG GTT AGG GT-**Cy5**	Biomers
5'Cy5_hTelo (mut)	Human telomer	DNA	**Cy5**-AAA ATT AAA ATT AAA ATT AAA AT	Sigma
5'Cy5_sp18_cKit1	Human *c-kit* gene promoter	DNA	**Cy5**-**6XPEG**-AGG GAG GGC GCT GGG AGG AGG G	Biomers
5'Cy5_cKit1	Human *c-kit* gene promoter	DNA	**Cy5**-AGG GAG GGC GCT GGG AGG AGG G	Biomers
3'Cy5_cKit1	Human *c-kit* gene promoter	DNA	AGG GAG GGC GCT GGG AGG AGG G-**Cy5**	Biomers
3'Cy5_sp18_cKit1	Human *c-kit* gene promoter	DNA	AGG GAG GGC GCT GGG AGG AGG G-**6XPEG**-**Cy5**	Biomers
5'Cy5_cMyc	Human *c-Myc* gene promoter	DNA	**Cy5**-TGG GGA GGG TGG GGA GGG TGG GGA AGG	Biomers
3'Cy5_cMyc	Human *c-Myc* gene promoter	DNA	TGG GGA GGG TGG GGA GGG TGG GGA AGG-**Cy5**	Biomers
5'DY647_NRAS	Human NRAS 5'UTR	RNA	**DY647**-UGU GGG AGG GGC GGG UCU GGG	Biomers
hTelo (wt)	Human telomer	DNA	AGG GTT AGG GTT AGG GTT AGG GT	Sigma
hTelo (mut)	Human telomer	DNA	AAA ATT AAA ATT AAA ATT AAA AT	Sigma
cKit1	Human *c-kit* gene promoter	DNA	AGG GAG GGC GCT GGG AGG AGG G	Sigma
dsDNA1	n.a.	DNA	**Cy5**-CAA TCG GAT CGA ATT CGA TCC GAT TG	Biomers
dsDNA2	n.a.	DNA	**Cy5**-ACA GTA GAG ATG CTG CTG ATT CGT TCA TGT GCT TCA AGC	Biomers
			comp: GCT TGA AGC ACA TGA ACG AAT CAG CAG CAT CTC TAC TGT	Biomers
dsDNA3	n.a.	DNA	**Cy5**-**6XPEG**-ACA GTA GAG ATG CTG CTG ATT CGT TCA TGT GCT TCA AGC	Biomers
			comp: GCT TGA AGC ACA TGA ACG AAT CAG CAG CAT CTC TAC TGT	Biomers

Table S1. List of oligonucleotides used in this study. Cy5 = Cyanine dye (ex: 650 nm/ em: 670 nm), DY647 = Cy5 analog (ex: 653 nm/ em: 672 nm), 6XPEG = hexaethylene glycol linker, comp = complementary sequence.

Table S2:

Oligo name	Sequence (modification in bold)	Dissociation constant, µM	Method	Reference
NRAS	**DY647**-UGU GGG AGG GGC GGG UCU GGG	0.21 ± 0.01	Quench	Present
	FAM-UGU GGG AGG GGC GGG UCU GGG-**TAMRA**	0.13 ± 0.03	FRET quench	S1
cKit1	**Cy5**-AGG GAG GGC GCT GGG AGG AGG G	1.3 ± 0.2	Quench	Present
	AGG GAG GGC GCT GGG AGG AGG G-**Cy5**	0.17 ± 0.01	Quench	Present
	GGG AGG GCG CTG GGA GGA GGG	(a) 0.067 ± 0.007, (b) 1 .0 ± 0.1	ITC	S2
	Bio-TTT TTT TTT GGG AGG GCG CTG GGA GGA GGG	(a) 0.067 ± 0.009, (b) 0.27 ± 0. 04	SPR	S2
	GGG AGG GCG CTG GGA GGA GGG	(a) 0.071 ± 0.004, (b) 2 .00 ± 0.08	UV-Vis	S2
cMyc	**Cy5**-TGG GGA GGG TGG GGA GGG TGG GGA AGG	0.015 ± 0.003	Quench	Present
	TGG GGA GGG TGG GGA GGG TGG GGA AGG-**Cy5**	0.31 ± 0.02	Quench	Present
	GGG GAG GGT GGG GAG GGT GGG G	(a) 0.014 ± 0.001, (b) 1.0 ± 0.1	ITC	S2
	TGG GGA GGG TGG GGA GGG TGG GGA AGG	(a) 0.091 ± 0.008, (b) 4.3 ± 0.2	ITC	S3
	TGG GGA GGG TGG GGA GGG TGG GGA	(a) 0.20 ± 0.02, (b) 5.0 ± 3.0	ITC	S4
	Bio-TTT TTT TTT GGG GAG GGT GGG GAG GGT GGG G	(a) 0.033 ± 0.004, (b) 0.25 ± 0.04	SPR	S2
	GGG GAG GGT GGG GAG GGT GGG G	(a) 0.0106 ± 0.0006, (b) 0.91 ± 0.04	UV-Vis	S2
hTelo	**Cy5**-AGG GTT AGG GTT AGG GTT AGG GT	1.9 ± 0.2	Quench	Present
	AGG GTT AGG GTT AGG GTT AGG GT-**Cy5**	0.15 ± 0.01	Quench	Present
	AGG GTT AGG GTT AGG GTT AGG GT	(a) 0.020 ± 0.001, (b) 0.25 ± 0.01	ITC	S5
	GGG TTA GGG TTA GGG TTA GGG	(a) 0.25 ± 0.03, (b) 2.0 ± 0.2	ITC	S2
	Bio-TTT TTT TTT GGG TTA GGG TTA GGG TTA GGG	(a) 0.20 ± 0.03, (b) 0.50 ± 0.08	SPR	S2
	Bio-AGG GTT AGG GTT AGG GTT AGG G	0.05 ± 0.01	SPR	S6
	GGG TTA GGG TTA GGG TTA GGG TT-peptide-**Bio**	0.81	SPR	S7
	GGG TTA GGG TTA GGG TTA GGG TT-peptide-**Bio**	0.51	SPR	S7
	GGG TTA GGG TTA GGG TTA GGG TT-peptide-**Bio**	0.76	SPR	S7
	GGG TTA GGG TTA GGG TTA GGG	(a) 0.20 ± 0.01, (b) 0.91 ± 0.04	UV-Vis	S2

Table S2. List of equilibrium binding constants compiled from literature and the present study. Cy5 = Cyanine dye (ex: 650 nm/ em: 670 nm), DY647 = Cy5 analog (ex: 653 nm/ em: 672 nm), TAMRA = tetramethylrhodamine dye (ex: 565 nm/ em: 580 nm), FAM = fluorescein dye (ex: 494 nm/ em: 518 nm), Bio = biotin label.

Figure S1:

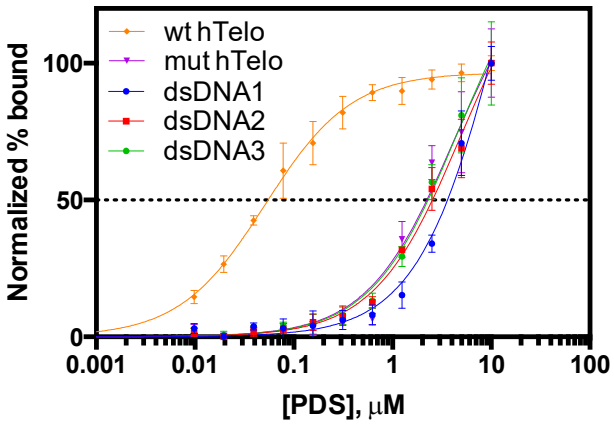

Figure S1. Comparison of G4 DNA, ssDNA, and dsDNA. All constructs contain 5'Cy5 label.

Figure S2:

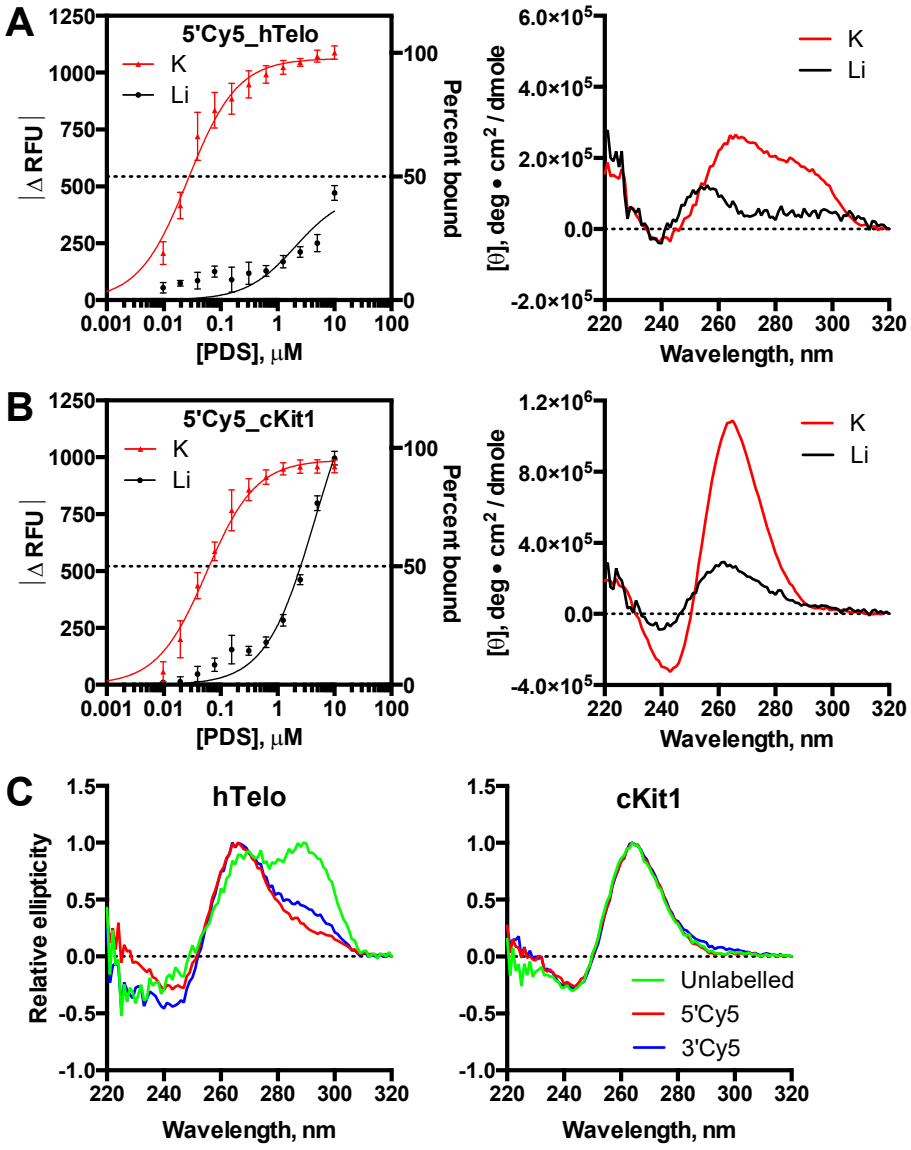

Figure S2. Cation-dependent fluorescence quenching and corresponding CD spectra. The degree of fluorescence quenching is proportional to the extent of G4 formation. A) hTelo sequence, B) cKit1 sequence. C) CD spectra of labelled and unlabelled hTelo and cKit constructs. Labelled hTelo exhibits fluorophore-induced parallel G4 conformation.

Figure S3:

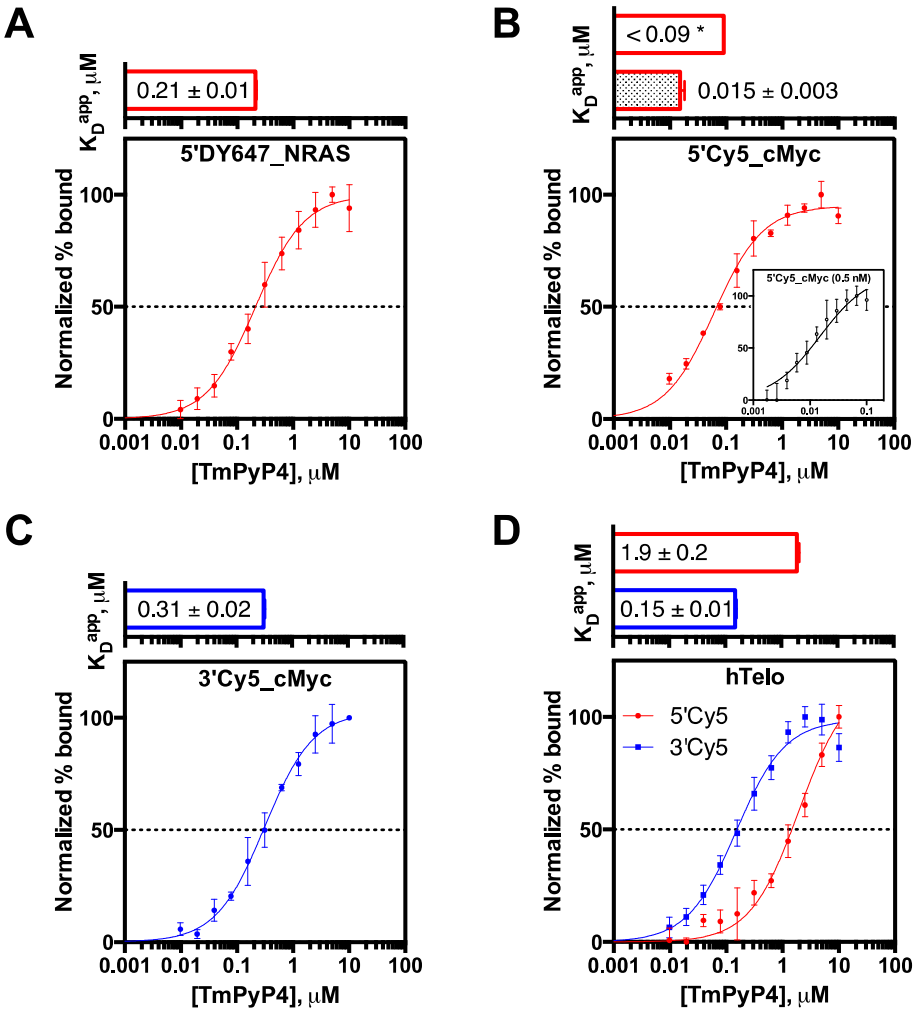

Figure S3. Equilibrium dissociation binding curves for TmPyP4. Red = 5'-end label and blue = 3'-end label. A) NRAS sequence, B) 5'Cy5_cMyc sequence (inset: 0.5 nM oligo conditions to avoid ligand depletion that significantly alters $[ligand]_{bound}$:$[ligand]_{unbound}$. Samples scaled to 300 µL to increase signal intensity. Bar graph shading = data from inset.), C) 3'Cy5_cMyc sequence, D) G-tetrad selective binding with hTelo sequence.

Figure S4:

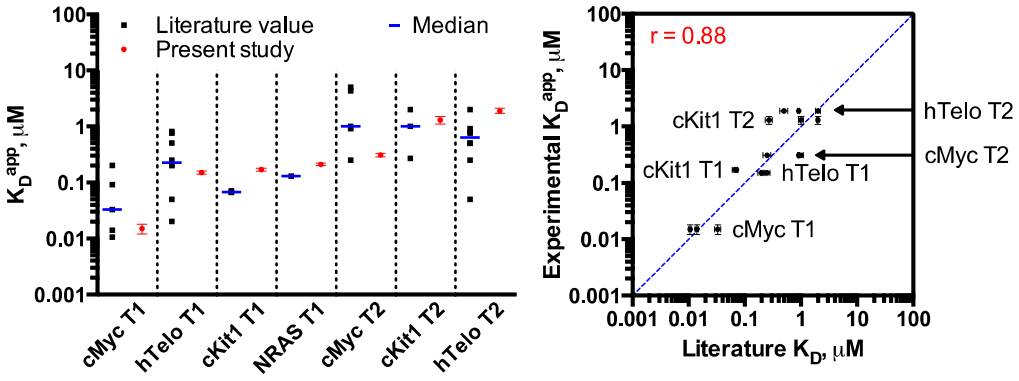

Figure S4. Cross-validation with literature values. A) Compilation of binding data (median of literature values shown with blue horizontal line). B) Pearson correlation analysis. T1 = high-affinity binding transition. T2 = low-affinity binding transition.

Note: Based on the apparent G-tetrad selectivity of TmPyP4, current measurements are in agreement with available literature values displayed in Figure S4. Compared to the reported values derived from equivalent conditions across several sequence constructs, the measured K_D^{app} values are in good correlation across a concentration range spanning approximately three orders of magnitude (r = 0.88). Overall, these data indicate that the assay described here accurately measures mutually exclusive ligand binding at G4 ends, caused by fluorophore quenching proximal to a given G-tetrad.

Figure S5:

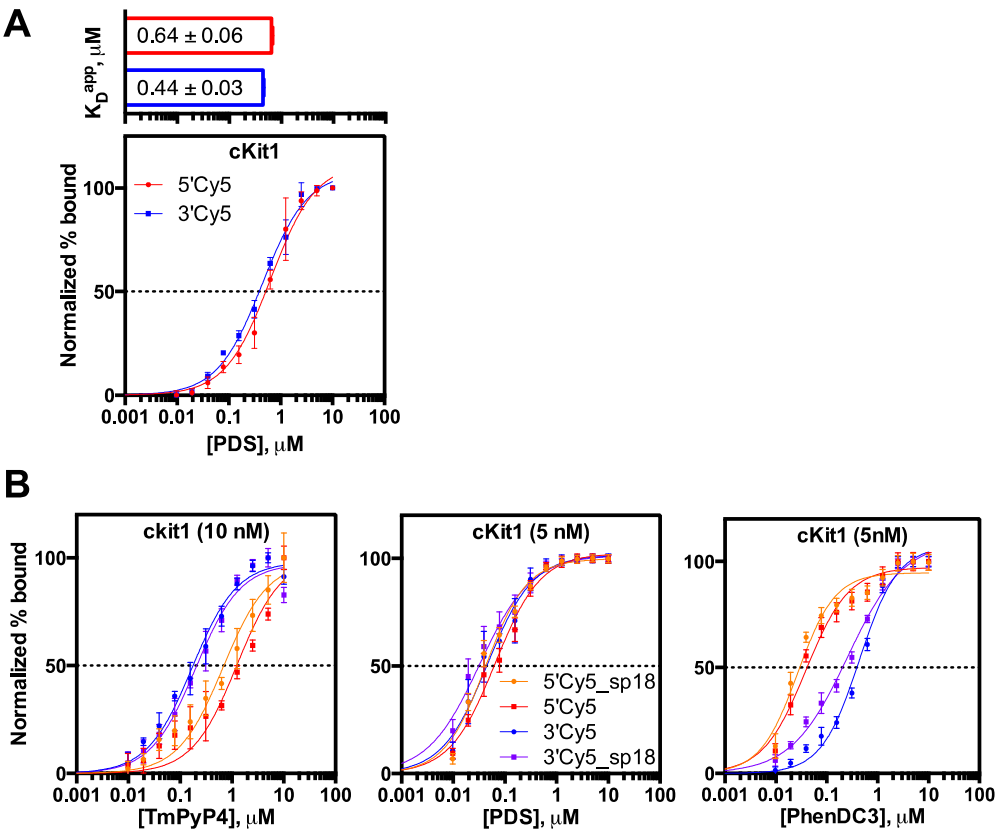

Figure S5. G-tetrad selectivity of cKit1 sequence. A) PDS shows equivalent G-tetrad selectivity with cKit1 sequence. B) Directly end-labelled and PEG linker-separated (sp18) labelled structures show little difference in G-tetrad selectivity of ligands.

General experimental procedures

All solvents and reagents were purified by standard techniques reported in Armarego, W. L. F., Chai, C. L. L., Purification of Laboratory Chemicals, 5th edition, Elsevier, 2003; or used as supplied from commercial sources (Sigma-Aldrich Corporation unless stated otherwise). NMR spectra were acquired on Bruker DRX-400, Bruker DPX-400 and DRX-500 instruments using deuterated solvents as detailed and at ambient probe temperature (300 K). Notation for the ^{1}H NMR spectral splitting patterns includes: singlet (*s*), doublet (*d*), triplet (*t*), broad (*br*) and multiplet/overlapping peaks (*m*). Signals are quoted as δ values in ppm, coupling constants (*J*), are quoted in Hertz and approximated to the nearest 0.5. Data analysis for the nuclear magnetic resonance (NMR) spectra was performed using MestReNova software. Mass spectra were recorded on a Micromass Q-Tof (ESI) spectrometer. Thin layer chromatography (TLC) was performed on Merck Kieselgel 60 F254 plates, and spots were visualized under UV light. Flash chromatography (FC) was performed using Merck Kieselgel 60 at room temperature under a positive pressure of nitrogen using previously distilled solvents. High performance liquid chromatography (HPLC) purification was carried out on all final compounds by using a Varian Pursuit C18, 5 μ column (250 × 21.2 mm) and a gradient elution with H_2O / acetonitrile (MeCN) containing 0.1% TFA at a flow rate of 20.0 ml/ min. All cellular assays have been performed with final compounds which had a purity of ≥98% according LC-MS analysis.

Typical binding assay (4 replicates): To 5 mL of assay buffer (50 mM TrisHCl, pH 7.2, 150 mM KCl, 0.5 w/v % CHAPS, 0.05 v/v % Triton X-100) was added 0.5 μL of 100 μM labeled oligo solution; thus, the resultant concentration of oligo was 10 nM. To anneal the oligo, the solution was heated to 95 °C for 5 min, then it was placed at 4 °C for 15 min, or until the solution reached 20 °C (room temperature). During the cooling step, a ligand dilution series was prepared: 50 μL of 100 μM ligand in 0.1 v/v % DMSO and water was used as the initial concentration. Subsequent 1:1 serial dilutions were made by adding 50 μL of 0.1 v/v % DMSO in water to the same volume of ligand solution, resulting in a total of 12 concentrations (including a no-compound control). Then, 10 μL per solution of the dilution series was transferred to a 12-well row within a 96-well PCR plate (Bio-Rad white-walled, skirted, low-profile, 96-well PCR plate). This was repeated four times to create four replicate rows containing the same dilution series. To these wells was added 90 μL aliquots of the aforementioned annealed oligo solution (final [oligo] = 9 nM). The wells were sealed with an adhesive foil cover and placed on an orbital plate shaker for gentle agitation (caution: set shaker to avoid splashing well contents on adhesive cover) at room temperature for 2 hr. Then, end-point fluorescence of each well was measure on either a qPCR instrument (Bio-Rad CFX96 Touch) or a fluorescence plate reader (BMG PHERAstar Plus). The differences in RFU were converted to absolute values relative to the no-compound control (DMSO control). The range of observed absolute RFU change was used to normalize the measurements in terms of % bound. These values were used as inputs in a one-site binding model (GraphPad Prism V.6) for curve fitting. Variance reported at standard error of the mean (SEM).

Circular dichroism analysis: 200 µL of 10 µM oligo were prepared in assay buffer. The oligo was annealed as described above. Then, the solution was transferred to a 1.00 mm cuvette and topped with 100 µL of mineral oil. The sample was analysed at room temperature using an Applied Photophysics Chirascan Plus circular dichrometer (spectrum scan, 1 nm interval, 10 averaged replicates). The reported spectra were baseline-corrected relative to buffer control.

Synthesis:
Pyridostatin (PDS): 4-(2-aminoethoxy)-N2,N6-bis(4-(2-aminoethoxy)quinolin-2-yl)pyridine-2,6-dicarboxamide. Synthesis as described by Rodriguez *et al.*[S8]

TmPyP4: 5,10,15,20-Tetrakis(1-methyl-4-pyridinio)porphyrin tetra(p-toluenesulfonate). Commercially available at Sigma (SKU 323497)

PhenDC3: 3,3'-((1,10-phenanthroline-2,9-dicarbonyl)bis(azanediyl))bis(1-methylquinolin-1-ium). Synthesis as described by De Cian *et al.*[S9]

References

(S1) M. Faudale, S. Cogoi, L. E. Xodo, *Chem. Commun.,* 2012, **48**, 874-6.
(S2) A. Arora, S. Maiti, *J. Phys. Chem. B*., 2008, **112**, 8151-59.
(S3) M. W. Freyer, R. Buscaglia, K. Kaplan, D. Cashman, L. H. Hurley, E. A. Lewis, *Biophys. J.,* 2007, **92**, 2007-15.
(S4) J. M. Dettler, R. Buscaglia, V. H. Le, E. A. Lewis, *Biophys. J.,* 2011, **100**, 1517-25.
(S5) L. Martino, B. Pagano, I. Fotticchia, S. Neidle, C. Giancola, *J. Phys. Chem. B*., 2009, **113**, 14779-86.
(S6) E. W. White, F. Tanious, M. A. Ismail, A. P. Feszka, S. Neidle, D. W. Boykin, W. D. Wilson, *Biophys. Chem.,* 2007, **126**, 140-53.
(S7) P. Murat, R. Bonnet, A. Van der Heyden, N. Spinelli, P. Labbé, D. Monchaud, M. P. Teulade-Fichou, P. Dumy, E. Defrancq, *Chem. Eur. J.,* 2010, **16**, 6106-14.
(S8) R. Rodriguez, S. Müller, J. A. Yeoman, C. Trentesaux, J. F. Riou, S. Balasubramanian, *J. Am. Chem. Soc.,* 2008, **130**, 15758-9.
(S9) A. De Cian, E. Delemos, J. L. Mergny, M. P. Teulade-Fichou, D. Monchaud, *J. Am. Chem. Soc.,* 2007, **129**, 1856-7.